A M-cadherin | Ki67 | DAPI | Merge
Cont
AFS98
50

B

C Cont IgG (GK1.5) | AFS98
H.E
eMyHC

D

E

F 1d | 3d | 7d | 10d | 14d
Cont
AFS98
SM/C-2.6
CD31/CD45/Sca-1

G

H M-cadherin | M-cadherin DAPI
Cont
AFS98

Fig. 5 – AFS98-treated regenerating muscles exhibit severe muscle fibrosis. CTX-treated TA muscles from day 14 were sampled, and the sections were visualized by Masson trichrome staining. The control TA muscle (A) showed normal muscle regeneration, but AFS98-treated TA muscle (B) exhibited impaired muscle regeneration. Scale bar: 400 μm. C and D are close-up images of the squares in A and B, respectively. Light blue represents fibrosis. Scale bar: 100 μm.

0.56×10^6 cells, respectively. These results indicate that acute macrophage-specific suppression led to the severe skeletal muscle regeneration defect.

No expression of M-CSF receptor on primary myoblasts

To investigate whether M-CSF directly affects myogenic cells, we examined expression of the M-CSF receptor (M-CSFR) on primary myoblasts. Macrophages (F4/80⁺) in the peritoneal exudate cells

(PEC) expressed M-CSFR (Fig. 3A), but neither C2/4, a subclone of C2C12, nor primary myoblasts expressed M-CSFR. We also examined the M-CSFR expression in skeletal muscle at 3 days after CTX injection, and found that M-CSFR did not co-exist with M-cadherin, a satellite cell/myoblast marker [24] (Fig. 3B). Moreover, the presence of M-CSF did not change the BrdU uptake of primary myoblasts (Fig. 3C). These results clearly indicate that M-CSF/M-CSFR signaling did not directly affect myogenic cell proliferation either in vitro or in vivo.

Fig. 4 – Myoblast proliferation and differentiation are affected in AFS98-treated TA muscles. (A) TA muscles from control (PBS) (upper) and AFS98-treated (lower) mice were obtained 3 days after CTX injection, and the sections were stained by anti-M-cadherin (red) and Ki-67 (green) antibodies. Nuclei were stained with DAPI. Arrowheads indicate Ki67, M-cadherin double-positive cells. Scale bar: 50 μm. (B) The number of M-cadherin⁺ cells/field or the percentage of Ki-67⁺ cells in M-cadherin⁺ cells 3 days after CTX injection was counted in 11 to 21 randomly selected fields in the regenerating area. Closed and open columns show PBS- ($n=3$) and AFS98-treated ($n=5$) mice, respectively. The average is shown with SD. **$P<0.05$ (t-test). (C) TA muscles from control IgG (GK1.5: a and b)- and AFS98-treated (c and d) mice were obtained 4 days after CTX injection, and the sections were stained by eMyHC (red: b and d). Serial sections (a) and (c) were stained with H.E. Scale bar: 100 μm. (D) The number of eMyHC⁺ myofibers/field 4 days after CTX injection was calculated in 20 to 25 randomly selected fields in regenerating areas of 4 to 6 TA muscles. The average is shown with SD. *$P<0.01$ (t-test). (E) The areas of eMyHC⁺ myofibers in C were measured. The solid line shows the control IgG-treated result, and the dashed line is the result for AFS98-treated mice. (F) Representative FACS profiles of SM/C-2.6(+) CD31(−) CD45(−) Sca-1(−) cells (myogenic cells) during skeletal muscle regeneration. The number in the upper left of each FACS profile indicates the percentage of myogenic cells. (G) TA, GC, and Qu muscles of PBS (control) (solid line) and AFS98-treated (dashed line) mice were injected with CTX, and muscle-derived mononuclear cells from the regenerating muscles were stained with SM/C-2.6, anti-CD31, CD45, or Sca-1 antibodies. The horizontal axis indicates the time after CTX injection. The vertical axis shows the mean number of satellite cells/myoblasts with SD. Three mice were used for each sample. *$P<0.01$ (t-test). (H) TA muscles from control (PBS) (upper) and AFS98-treated (lower) mice were obtained 7 days after CTX injection, and the sections were stained by anti-M-cadherin (green) antibody. Nuclei were counterstained with DAPI. Arrowheads show M-cadherin-positive cells. Scale bar: 50 μm. The graph shows the number of M-cadherin⁺ cells/field. Closed and open columns show PBS- and AFS98-treated mice, respectively. Three TA muscles were used for each sample. The average is shown with SD. **$P<0.05$ (t-test).

Inhibition of satellite cell proliferation and myotube formation by macrophage depletion

To clarify whether the number of proliferating satellite cells was decreased or not in the macrophage-suppressed condition, we stained sections of AFS98-treated TA muscles 3 days after CTX injection. As shown in Fig. 4A, M-cadherin-positive mononuclear cells were observed in the control muscles, whereas M-cadherin-positive cells were significantly fewer in the AFS98-treated muscles (Fig. 4B and Supplemental Table I). Moreover, Ki67-positive proliferating satellite cells were significantly decreased in AFS98-treated mice (Figs. 4A and B). These results indicate that the suppression of macrophages led to a decrease in the number of proliferating satellite cells in vivo.

We next examined myotube formation in these mice. At day 4 after CTX injection, muscles injected with the control antibody (GK1.5, anti-CD4: rat IgG) showed many newly formed myotubes with embryonic myosin heavy chain (eMyHC) expression (Fig. 4C). There was no obvious difference between GK1.5- and PBS-treated mice (Fig. 1A). On the other hand, small myotubes were widely dispersed in AFS98-treated mice (Fig. 4C). Fig. 4D shows the difference between the percentages of eMyHC-positive myotube areas in GK1.5- and AFS98-treated muscles. About 45% of fields had more than 20% of eMyHC-positive myotube in the control mice, but we never detected such area in the AFS98-treated mice. Moreover, the eMyHC-positive myotubes in AFS98-treated mice were smaller than those in GK1.5-treated muscle (Fig. 4E). Similar results were obtained in a freeze-injury model that showed clearly separated uninjured and injured areas (Supplemental Fig. 1).

We then examined the time course of myogenic cell production using SM/C-2.6, anti-CD31, CD45, and Sca-1 mAbs by FACS [16,25]. Myogenic cells from the regenerating muscle were highly enriched in the SM/C-2.6(+) CD31(−) CD45(−) Sca-1(−) fraction (Supplemental Figs. 2 and 3). As shown in Figs. 4F and G, SM/C-2.6(+) CD31 (−) CD45(−) Sca-1(−) satellite/myogenic cells were increased and reached a peak on day 3 in PBS-treated mice. In AFS98-treated mice, however, muscle satellite/myogenic cells increased, but they reached a peak on day 7, suggesting delayed proliferation of satellite cells compared to control muscles (Fig. 4G). In fact, the number of M-cadherin-positive cells of AFS98-treated mice was higher than that of PBS-treated mice at 7 days after CTX injection (Fig. 4H and Supplemental Table I). These results indicate that macrophage-specific depletion in vivo affected both the proliferation and differentiation of satellite cells.

Severe defect of muscle regeneration in AFS98-treated muscle

At day 14 after CTX injection, the PBS-injected control muscle showed regenerating fibers with central nuclei (Figs. 5A and C), however, the AFS98-injected group indicated many necrotic fibers and interstitial areas. It is evident from the Masson trichrome staining that interstitial spaces between the necrotic fibers were enlarged and that severe fibrosis was present (Figs. 5B and D). In addition, accumulations of adipocytes were also observed in AFS98-treated muscle (Supplemental Fig. 4). We could detect necrotic fibers and adipocytes at least 21 days after cardiotoxin injection (data not shown). These results indicate that muscle regeneration requires functioning macrophages and that both fibrosis and adipogenesis are induced in the absence of macrophages.

## Up-regulation of molecules related to fibrosis generation in AFS98-treated muscle

We then focused on the question of how fibrosis was generated in the muscles lacking macrophages. TA muscles of control and AFS98-treated mice were obtained, and fibrosis-related molecules were examined using quantitative RT-PCR. As shown in Fig. 6A, mRNA expression of connective tissue growth factor (CTGF) in control TA muscles was not very different at any time point tested. On the other hand, CTGF mRNA in the AFS98-treated TA muscles was increased significantly on days 3 to 14. At the same time, using cDNAs, like the CTGF mRNA measurement, collagen type I mRNA was measured by quantitative PCR and was found to be significantly elevated on day 7 (Fig. 6A) in AFS98-treated TA muscles. We also demonstrated the mRNA expression of the fibrosis mediators TGF-β1–3. Intriguingly, TGF-β3 was the most increased molecule. On the other hand, TGF-β1 was not very much up-regulated in the AFS98-treated mice.

Expressions of collagen type I proteins were examined immunohistochemically. As shown in the Fig. 6B, collagen type I expression was more significantly up-regulated in the AFS98-treated TA muscles than in control muscles. These results indicate that a macrophage-independent mechanism induced fibrosis-related molecules and led to muscle fibrosis.

Expression of fibrosis markers in CD90-positive fraction

In AFS98-treated mice, the total cell number was decreased until 3 days after CTX injection. However, the total number of

---

Fig. 6 – Fibrosis markers are up-regulated in AFS98-treated mice. (A) TA, Qu, and GC muscles were isolated from control (PBS, black columns) or AFS98-treated (white columns) mice, and the expressions of five fibrosis markers were evaluated by real-time PCR. The horizontal axis indicates the number of days after CTX injection. The vertical axis shows the relative expression of each gene with SD. *$P < 0.01$, **$P < 0.05$ (t-test). N.D. means not determined. **(B)** TA muscle sections (CTX-14d) from control (PBS) (a) and AFS98-treated (b) mice were stained with anti-collagen (red) antibodies. A serial section of (b) was stained with H.E. (c). Scale bar: 100 μm. **(C)** Representative FACS profiles of CD90(+) CD31(−) CD45(−) cells during skeletal muscle regeneration. The number in upper left of each FACS profile indicates the percentage of CD90(+) CD31(−) CD45(−) cells. **(D)** TA, GC, and Qu muscles of control (PBS) (solid line) and AFS98-treated (dashed line) mice were injected with CTX, and mononuclear cells from the regenerating muscles were stained with anti-CD90, CD31, and CD45 antibodies and analyzed by FACS. The horizontal axis indicates days after CTX injection. The vertical axis shows the mean numbers of CD90(+) CD31(−) CD45(−) cells with SD. Three mice were used for each sample. *$P < 0.01$, **$P < 0.05$ (t-test). **(E)** CD90(+) or CD90(−) cells were isolated from control (PBS, closed columns) or AFS98-treated (open columns) mice 7 days after CTX injection, and the expressions of five fibrosis markers were evaluated by real-time PCR. The horizontal axis indicates the cell type. The vertical axis shows the relative expression of each gene with SD.
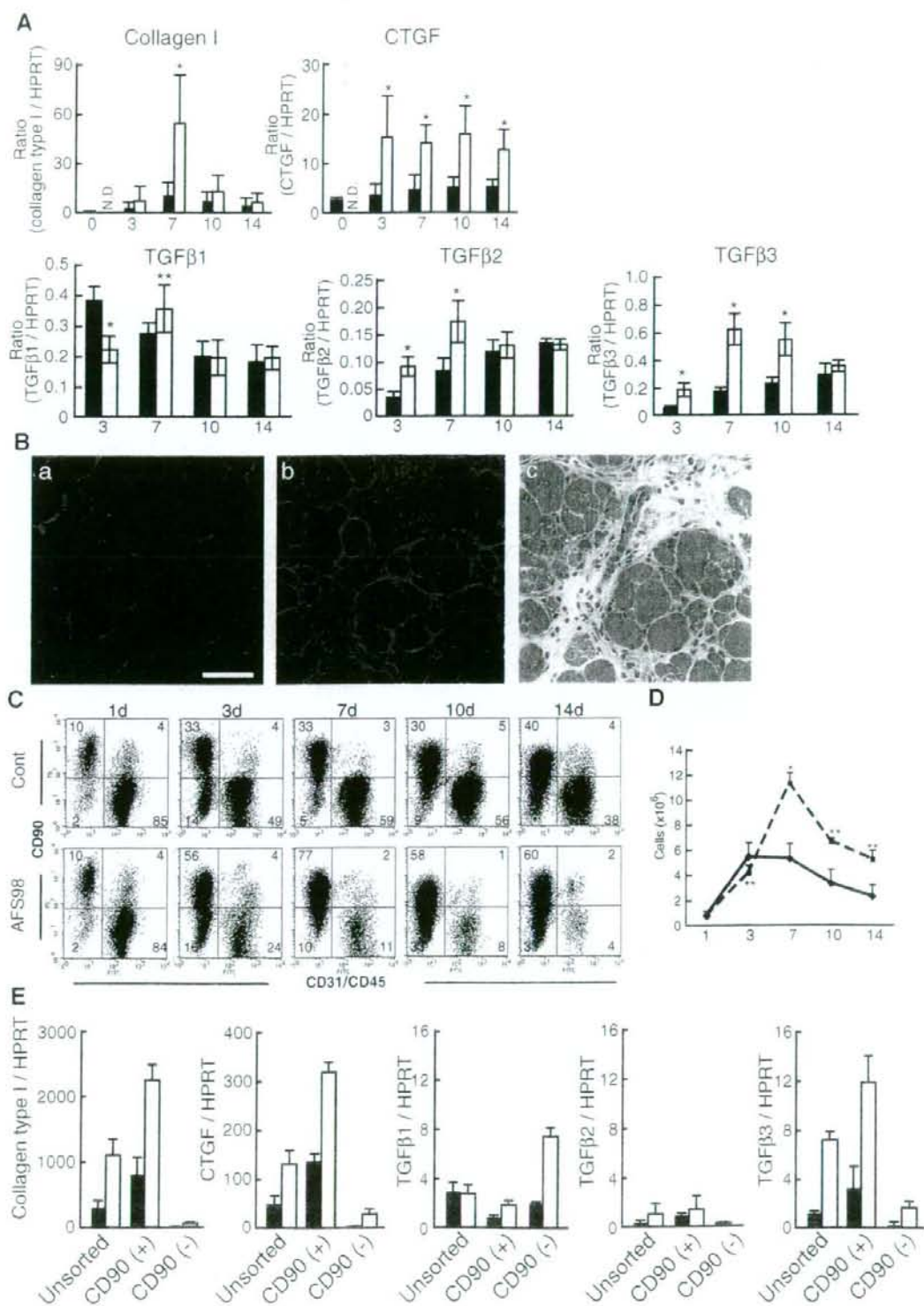
cells in AFS98-treated mice 7 days after CTX injection was similar to that in the control mice (Fig. 2B). To investigate the relationship between this result and the fibrosis, we focused on the CD90(+) CD31(−) CD45(−) cells that we recently described [16]. The physiological roles of CD90(+) CD31(−) CD45(−) cells are largely unknown, but the cell number of CD90(+) CD31(−) CD45(−) cells was temporarily increased during normal skeletal muscle regeneration (Figs. 6C and D) [16]. Furthermore, CD90(+) CD31(−) CD45(−) cells 3 days after CTX injection do not include myogenic cells [16]. Intriguingly, as shown in Figs. 6C and D, the number of CD90(+) CD31(−) CD45(−) cells in the AFS98-treated mice was higher than that in the PBS-treated mice 7 to 14 days after CTX injection. In addition, the up-regulated fibrosis-related molecules in Fig. 6A were enriched in the CD90(+) fraction (Fig. 6E). These results suggest that both the cell number and the gene expression of CD90(+) cells are also affected by macrophages and that CD90 (+) cells might be one index of muscle fibrosis.

Discussion

M-CSF signaling during skeletal muscle regeneration

M-CSF is known to play a key role in the differentiation and proliferation of macrophage/monocyte lineage cells. M-CSF production is genetically defective in osteopetrotic (*op/op*) mice [26,27] and is associated with defective osteoclast differentiation, which causes osteopetrosis. Previously, Dhawan et al. reported that *op/op* mice had normal skeletal muscle regeneration capability [28]. They also suggested that unidentified M-CSF-independent factors are capable of generating macrophages. We could not exactly explain the discrepancy between *op/op* and AFS98-treated mice, however, increased neutrophils or other cytokine might compensate for M-CSF in *op/op* mice.

Macrophages and skeletal muscle regeneration

The roles of macrophages in muscle regeneration have been studied by several investigators. CCR2 is a chemokine receptor with potent macrophage recruiting and activating functions [14]. Recent studies showed that CCR2-null mice exhibited impaired muscle regeneration, altered inflammation, and increased fat accumulation [15,29]. On the other hand, Shireman et al. reported that MCP-1 (a ligand of CCR2)-deficient mice exhibited impaired muscle regeneration similar to that of CCR2-null mice [30]. In CCR2-deficient mice, neither the expression of MyoD by proliferating myoblasts nor the expression of myogenin by differentiating myoblasts was altered [15]. In addition, although MyoD and myogenin are specifically expressed in cells committed to myogenesis [31], Summan et al. showed that MyoD and myogenin mRNA expressions were not different in macrophage-suppressed and control mice in a study using a clodronate-containing liposome [32]. These results imply that the numbers of satellite cells/myoblasts in macrophage-suppressed model mice were unchanged. However, as shown in Fig. 4, AFS98-treated mice showed a decreased number of satellite cells/myoblasts in the macrophage-depleted condition. Fewer newly formed myotubes were also observed. Furthermore, these mice showed a severe regeneration defect with muscular fibrosis (Figs. 5 and 6). It is

unclear why our and other models produced incongruent results, but it is possible that neutrophils compensated for the lack of macrophages because an increased number of neutrophils was observed in MCP-1-deficient regenerating muscle [30]. On the other hand, AFS98-treated mice did not show an increment of neutrophils during skeletal muscle regeneration (Fig. 2). These results suggest that the increased number of neutrophils might compensate for the loss of macrophages.

Recently, heterogeneity of macrophages was reported during skeletal muscle regeneration *in vivo*. Gr-1(+) CX3CR1(low) F4/80(+) inflammatory macrophages first appeared in the early stage of regeneration. Then, Gr-1(−) CX3CR1(high) F4/80 (high) anti-inflammatory macrophages were found in the middle to late stages [33]. These results suggest that Gr-1(+) CX3CR1(low) F4/80(+) and Gr-1(−) CX3CR1(high) F4/80(high) macrophages may play roles in myoblast proliferation and differentiation *in vivo*, respectively. The macrophage-depletion models reported here showed significant decreases of F4/80-positive macrophages throughout the regeneration. These results suggest that M-CSF/M-CSFR signaling is necessary for the generation of both Gr-1(+) CX3CR1(low) F4/80(+) and Gr-1(−) CX3CR1(high) F4/80(high) macrophages.

Macrophages and fibrosis

Like other macrophage-depletion models, the models reported here showed an increase in adipocytes in skeletal muscle (Fig. 5 and Supplemental Fig. 4) [15,32]. In addition, we observed that severe fibrosis and fibrosis-related molecules were up-regulated in AFS98 mAb-mediated macrophage-depleted mice. Warren et al. reported that the increased fibrosis in CCR2-null mice after freeze-injured. In contrast to our results, however, CCR2-null mice indicated a prolonged period of macrophage accumulation [15]. Macrophages are generally considered to be pro-fibrotic cells and TGF-β has been implicated as a key molecule in fibrosis [34]. As well as other tissues, it has been reported that macrophages are a potential source of TGF-β in skeletal muscle [35]. It is still unknown why up-regulation of these markers has been observed in macrophage-suppressed mice. Although Morrison et al. showed the relationship between T cells and muscle fibrosis, we could not observed T-cell accumulation in AFS98-treated mice (Supplemental Fig. 5) [36]. Therefore our results clearly indicate that there is a macrophage-independent fibrosis in skeletal muscle.

Fibrosis markers in macrophages-deficient mice

In contrast to collagen type I expression, continuous high expression of CTGF was observed in AFS98 mAb-treated regenerating muscles. CTGF is a member of the family of connective tissue growth factor-cysteine-rich 61-nephroblastoma overexpressed genes. It is known that CTGF is implicated in multiple cellular events, including fibrosis, and is a downstream effecter molecule mediating the action of TGF-β1, a cytokine known to induce severe and progressive fibrosis. In addition, it was reported that CTGF directly bound TGF-β1 and enhanced TGF-β1 signaling [37]. It is also interesting to note that both the mRNA expression levels and the changes in TGF-β3 levels were highest among the TGFβ-family (β1 to β3). It is still unknown why TGF-β3, but not TGF-β1, was up-regulated in our studies. However, these results suggest that CTGF might be enhanced by TGF-β3, resulting in severe muscle fibrosis. Finally, we found that CD90(+) CD31(−) CD45(−) cells were

continuously increased in AFS98-treated mice until day 7 after CTX injection. In addition fibrosis markers were strongly enriched in CD90(+) cells. We recently reported that CD90(+) cells 3 days after CTX injection do not include myogenic cells and that they produce laminin α2, a component of basal lamina [16]. These results suggest that CD90(+) CD31(−) CD45(−) cells might include precursors of fibroblast and these cells might play central roles of muscle fibrosis. The relationship between CD90(+) cells and fibrosis, as well as the physiological roles of CD90(+) cells during skeletal muscle regeneration, will be clarified in a future study.

In conclusion, we showed that macrophages were very important for the efficient proliferation and differentiation of satellite cells, and that M-CSF/M-CSFR signaling was important for the generation of macrophages during skeletal muscle regeneration. We also showed that CD90(+) CD31(−) CD45(−) cells were responsible for up-regulation of fibrosis-related molecules in AFS98-treated mice. Our findings facilitate the investigation of the relationship between macrophages and satellite cells during skeletal muscle regeneration.

Acknowledgments

Appendix A. Supplementary data

Supplementary data associated with this article can be found, in the online version, at doi:10.1016/j.yexcr.2008.08.008.

REFERENCES

[1] R. Bischof, Satellite and stem cells in muscle regeneration, in: A.G. Engel, C. Franzini-Armstrong (Eds.), Myology, 1, McGraw-Hill, New York, 2004, pp. 66–86.

[2] A. Mauro, Satellite cell of skeletal muscle fibers, J. Biophys. Biochem. Cytol. 9 (1961) 493–495.

[3] M.D. Grounds, Z. Yablonka-Reuveni, Molecular and cell biology of skeletal muscle regeneration, Mol. Cell Biol. Hum. Dis. Ser. 3 (1993) 210–256.

[4] E. Schultz, K.M. McCormick, Skeletal muscle satellite cells, Rev. Physiol. Biochem. Pharmacol. 123 (1994) 213–257.

[5] C.A. Collins, I. Olsen, P.S. Zammit, L. Heslop, A. Petrie, T.A. Partridge, J.E. Morgan, Stem cell function, self-renewal, and behavioral heterogeneity of cells from the adult muscle satellite cell niche, Cell 122 (2005) 289–301.

[6] S. Orimo, E. Hiyamuta, K. Arahata, H. Sugita, Analysis of inflammatory cells and complement C3 in bupivacaine-induced myonecrosis, Muscle Nerve 14 (1991) 515–520.

[7] T.A. Robertson, M.A. Maley, M.D. Grounds, J.M. Papadimitriou, The role of macrophages in skeletal muscle regeneration with particular reference to chemotaxis, Exp. Cell Res. 207 (1993) 321–331.

[8] M. Cantini, U. Carraro, Macrophage-released factor stimulates selectively myogenic cells in primary muscle culture, J. Neuropathol. Exp. Neurol. 54 (1995) 121–128.

[9] T.J. Hawke, D.J. Garry, Myogenic satellite cells: physiology to molecular biology, J. Appl. Physiol. 91 (2001) 534–551.

[10] C. Dogra, H. Changotra, S. Mohan, A. Kumar, Tumor necrosis factor-like weak inducer of apoptosis inhibits skeletal myogenesis through sustained activation of nuclear factor-kappaB and degradation of MyoD protein, J. Biol. Chem. 281 (2006) 10327–10336.

[11] M. Girgenrath, S. Weng, C.A. Kostek, B. Browning, M. Wang, S.A. Brown, J.A. Winkles, J.S. Michaelson, N. Allaire, P. Schneider, M.L. Scott, Y.M. Hsu, H. Yagita, R.A. Flavell, J.B. Miller, L.C. Burkly, T.S. Zheng, TWEAK, via its receptor Fn14, is a novel regulator of mesenchymal progenitor cells and skeletal muscle regeneration, Embo J. 25 (2006) 5826–5839.

[12] A. Hirata, S. Masuda, T. Tamura, K. Kai, K. Ojima, A. Fukase, K. Motoyoshi, K. Kamakura, Y. Miyagoe-Suzuki, S. Takeda, Expression profiling of cytokines and related genes in regenerating skeletal muscle after cardiotoxin injection: a role for osteopontin, Am. J. Pathol. 163 (2003) 203–215.

[13] L. Lescaudron, E. Peltekian, J. Fontaine-Perus, D. Paulin, M. Zampieri, L. Garcia, E. Parrish, Blood borne macrophages are essential for the triggering of muscle regeneration following muscle transplant, Neuromuscul. Disord. 9 (1999) 72–80.

[14] I.F. Charo, M.B. Taubman, Chemokines in the pathogenesis of vascular disease, Circ. Res. 95 (2004) 858–866.

[15] G.L. Warren, T. Hulderman, D. Mishra, X. Gao, L. Millecchia, L. O'Farrell, W.A. Kuziel, P.P. Simeonova, Chemokine receptor CCR2 involvement in skeletal muscle regeneration, Faseb J. 19 (2005) 413–415.

[16] S. Fukada, Y. Yamamoto, M. Segawa, K. Sakamoto, M. Nakajima, M. Sato, D. Morikawa, A. Uezumi, Y. Miyagoe-Suzuki, S. Takeda, K. Tsujikawa, H. Yamamoto, CD90-positive cells, an additional cell population, produce laminin alpha2 upon transplantation to dy (3k)/dy(3k) mice, Exp. Cell Res. 314 (2008) 193–203.

[17] T. Sudo, S. Nishikawa, M. Ogawa, H. Kataoka, N. Ohno, A. Izawa, S. Hayashi, S. Nishikawa, Functional hierarchy of c-kit and c-fms in intramarrow production of CFU-M, Oncogene 11 (1995) 2469–2476.

[18] S. Fukada, S. Higuchi, M. Segawa, K. Koda, Y. Yamamoto, K. Tsujikawa, Y. Kohama, A. Uezumi, M. Imamura, Y. Miyagoe-Suzuki, S. Takeda, H. Yamamoto, Purification and cell-surface marker characterization of quiescent satellite cells from murine skeletal muscle by a novel monoclonal antibody, Exp. Cell Res. 296 (2004) 245–255.

[19] S. Fukada, A. Uezumi, M. Ikemoto, S. Masuda, M. Segawa, N. Tanimura, H. Yamamoto, Y. Miyagoe-Suzuki, S. Takeda, Molecular signature of quiescent satellite cells in adult skeletal muscle, Stem Cells 25 (2007) 2448–2459.

[20] K. Ojima, A. Uezumi, H. Miyoshi, S. Masuda, Y. Morita, A. Fukase, A. Hattori, H. Nakauchi, Y. Miyagoe-Suzuki, S. Takeda, Mac-1(low) early myeloid cells in the bone marrow-derived SP fraction migrate into injured skeletal muscle and participate in muscle regeneration, Biochem. Biophys. Res. Commun. 321 (2004) 1050–1061.

[21] S. Fukada, Y. Miyagoe-Suzuki, H. Tsukihara, K. Yuasa, S. Higuchi, S. Ono, K. Tsujikawa, S. Takeda, H. Yamamoto, Muscle regeneration by reconstitution with bone marrow or fetal liver cells from green fluorescent protein-gene transgenic mice, J. Cell. Sci. 115 (2002) 1285–1293.

[22] A. Uezumi, K. Ojima, S. Fukada, M. Ikemoto, S. Masuda, Y. Miyagoe-Suzuki, S. Takeda, Functional heterogeneity of side population cells in skeletal muscle, Biochem. Biophys. Res. Commun. 341 (2006) 864–873.

[23] T. Murayama, M. Yokode, H. Kataoka, T. Imabayashi, H. Yoshida, H. Sano, S. Nishikawa, S. Nishikawa, T. Kita, Intraperitoneal administration of anti-c-fms monoclonal antibody prevents initial events of atherogenesis but does not reduce the size of advanced lesions in apolipoprotein E-deficient mice, Circulation 99 (1999) 1740–1746.

[24] A. Irintchev, M. Zeschnigk, A. Starzinski-Powitz, A. Wernig, Expression pattern of M-cadherin in normal, denervated, and regenerating mouse muscles, Dev. Dyn. 199 (1994) 326–337.

[25] M. Ikemoto, S. Fukada, A. Uezumi, S. Masuda, H. Miyoshi, H. Yamamoto, M.R. Wada, N. Masubuchi, Y. Miyagoe-Suzuki, S. Takeda, Autologous transplantation of SM/C-2.6(+) satellite cells transduced with micro-dystrophin CS1 cDNA by lentiviral vector into mdx mice, Mol. Ther. 15 (2007) 2178–2185.

[26] H. Yoshida, S. Hayashi, T. Kunisada, M. Ogawa, S. Nishikawa, H. Okamura, T. Sudo, L.D. Shultz, S. Nishikawa, The murine mutation osteopetrosis is in the coding region of the macrophage colony stimulating factor gene, Nature 345 (1990) 442–444.

[27] M. Naito, S. Hayashi, H. Yoshida, S. Nishikawa, L.D. Shultz, K. Takahashi, Abnormal differentiation of tissue macrophage populations in 'osteopetrosis' (op) mice defective in the production of macrophage colony-stimulating factor, Am. J. Pathol. 139 (1991) 657–667.

[28] J. Dhawan, T.A. Rando, S.E. Elson, F. Lee, E.R. Stanley, H.M. Blau, Myoblast-mediated expression of colony stimulating factor-1 (CSF-1) in the cytokine-deficient op/op mouse, Somat. Cell. Mol. Genet. 22 (1996) 363–381.

[29] V. Contreras-Shannon, O. Ochoa, S.M. Reyes-Reyna, D. Sun, J.E. Michalek, W.A. Kuziel, L.M. McManus, P.K. Shireman, Fat accumulation with altered inflammation and regeneration in skeletal muscle of CCR2−/− mice following ischemic injury, Am. J. Physiol. Cell. Physiol. 292 (2007) C953–967.

[30] P.K. Shireman, V. Contreras-Shannon, O. Ochoa, B.P. Karia, J.E. Michalek, L.M. McManus, MCP-1 deficiency causes altered inflammation with impaired skeletal muscle regeneration, J. Leukoc. Biol. 81 (2007) 775–785.

[31] S.B. Charge, M.A. Rudnicki, Cellular and molecular regulation of muscle regeneration, Physiol. Rev. 84 (2004) 209–238.

[32] M. Summan, G.L. Warren, R.R. Mercer, R. Chapman, T. Hulderman, N. Van Rooijen, P.P. Simeonova, Macrophages and skeletal muscle regeneration: a clodronate-containing liposome depletion study, Am. J. Physiol. Regul. Integr. Comp. Physiol. 290 (2006) R1488–1495.

[33] L. Arnold, A. Henry, F. Poron, Y. Baba-Amer, N. van Rooijen, A. Plonquet, R.K. Gherardi, B. Chazaud, Inflammatory monocytes recruited after skeletal muscle injury switch into antiinflammatory macrophages to support myogenesis, J. Exp. Med. 204 (2007) 1057–1069.

[34] T.A. Wynn, Cellular and molecular mechanisms of fibrosis, J. Pathol. 214 (2008) 199–210.

[35] L.E. Gosselin, J.E. Williams, M. Deering, D. Brazeau, S. Koury, D.A. Martinez, Localization and early time course of TGF-beta 1 mRNA expression in dystrophic muscle, Muscle Nerve 30 (2004) 645–653.

[36] J. Morrison, D.B. Palmer, S. Cobbold, T. Partridge, G. Bou-Gharios, Effects of T-lymphocyte depletion on muscle fibrosis in the mdx mouse, Am. J. Pathol. 166 (2005) 1701–1710.

[37] J.G. Abreu, N.I. Ketpura, B. Reversade, E.M. De Robertis, Connective-tissue growth factor (CTGF) modulates cell signalling by BMP and TGF-beta, Nat. Cell Biol. 4 (2002) 599–604.

MECHANISMS
OF
DEVELOPMENT

Reduced proliferative activity of primary POMGnT1-null myoblasts in vitro

Yuko Miyagoe-Suzuki[a,*], Nami Masubuchi[a,b], Kaori Miyamoto[a,b], Michiko R. Wada[a], Shigeki Yuasa[c], Fumiaki Saito[d], Kiichiro Matsumura[d], Hironori Kanesaki[e], Akira Kudo[e], Hiroshi Manya[f], Tamao Endo[f], Shin'ichi Takeda[a]

[a]Department of Molecular Therapy, National Institute of Neuroscience, National Center of Neurology and Psychiatry,
4-1-1 Ogawahigashi, Kodaira, Tokyo 187-8502, Japan
[b]Molecular Embryology, Department of Biosciences, School of Science, Kitasato University, Kanagawa 228-8555, Japan
[c]Department of Ultrastructural Research, National Institute of Neuroscience, National Center of Neurology and Psychiatry,
4-1-1 Ogawahigashi, Kodaira, Tokyo 187-8502, Japan
[d]Department of Neurology and Neuroscience, Teikyo University School of Medicine, 2-11-1 Kaga, Itabashi-ku, Tokyo 173-8605, Japan
[e]Department of Biological Information, Tokyo Institute of Technology, Yokohama 226-8501, Japan
[f]Glycobiology Research Group, Tokyo Metropolitan Institute of Gerontology,
Foundation for Research on Aging and Promotion of Human Welfare, 35-2 Sakaecho, Itabashi-ku, Tokyo 173-0015, Japan

ARTICLE INFO

ABSTRACT

Protein O-linked mannose β1,2-N-acetylglucosaminyltransferase 1 (POMGnT1) is an enzyme that transfers N-acetylglucosamine to O-mannose of glycoproteins. Mutations of the POMGnT1 gene cause muscle–eye–brain (MEB) disease. To obtain a better understanding of the pathogenesis of MEB disease, we mutated the POMGnT1 gene in mice using a targeting technique. The mutant muscle showed aberrant glycosylation of α-DG, and α-DG from mutant muscle failed to bind laminin in a binding assay. POMGnT1$^{-/-}$ muscle showed minimal pathological changes with very low-serum creatine kinase levels, and had normally formed muscle basal lamina, but showed reduced muscle mass, reduced numbers of muscle fibers, and impaired muscle regeneration. Importantly, POMGnT1$^{-/-}$ satellite cells proliferated slowly, but efficiently differentiated into multinuclear myotubes in vitro. Transfer of a retrovirus vector-mediated POMGnT1 gene into POMGnT1$^{-/-}$ myoblasts completely restored the glycosylation of α-DG, but proliferation of the cells was not improved. Our results suggest that proper glycosylation of α-DG is important for maintenance of the proliferative activity of satellite cells in vivo.

© 2008 Elsevier Ireland Ltd. All rights reserved.

1. Introduction

POMGnT1 is the glycosyltransferase that catalyzes the transfer of N-acetylglucosamine (GlcNAc) to O-mannose of glycoproteins, the second step of Ser/Thr O-mannosylation (Yoshida et al., 2001; reviewed in Endo and Toda, 2003). Mutations in the POMGnT1 gene cause muscle–eye–brain (MEB) disease, a rare autosomal recessive disorder characterized by congenital muscular dystrophy with elevated serum creatine kinase (CK) levels, severe visual failure, and gross mental retardation (Yoshida et al., 2001).

α-Dystroglycan (α-DG) is a heavily glycosylated glycoprotein and a well-known substrate of POMGnT1. Dystroglycan is encoded by a single gene (DAG1) and is cleaved into two proteins, α-dystroglycan (α-DG) and β-dystroglycan (β-DG), by posttranslational processing (Ibraghimov-Beskrovnaya et al., 1992). DGs are central components of the dystrophin-glycoprotein complex (DGC) at the sarcolemma, and α-DG was shown to serve as a cell surface receptor for laminin (Ibraghimov-Beskrovnaya et al., 1992), agrin (Gee et al., 1994; Campanelli et al., 1994), perlecan (Peng et al., 1998; Kanagawa et al., 2005), and neurexin (Sugita et al., 2001). In skeletal muscle, the laminin-α-DG linkage is thought to be critical for plasma membrane stability (recently reviewed in Kanagawa and Toda 2006). In MEB muscle, the α-DG core protein is preserved but hypo-glycosylated, and α-DG prepared from the muscle fails to bind laminin in vitro (Michele et al., 2002). Therefore, it is proposed that the disruption of the α-DG-laminin linkage is the main pathomechanism of dystrophic changes seen in MEB muscle.

To further elucidate the molecular pathogenesis of MEB disease, we generated POMGnT1-knockout mice using a gene targeting technique, and examined the mutant skeletal muscle. During our experiments, Liu et al. reported the generation of POMGnT1-deficient mice (Liu et al., 2006). The report showed severe muscle pathology, but the mechanism by which POMGnT1 deficiency causes muscle phenotype was not clearly shown. In this report, we report that POMGnT1-deficient mice show remarkably minimal signs of muscle degeneration and regeneration, but also show small muscle mass, reduced numbers of muscle fibers, and impaired muscle regeneration. POMGnT1-deficient myoblasts proliferate poorly in vitro. The proliferation was not improved by retrovirus vector-mediated POMGnT1 expression in POMGnT1$^{-/-}$ myoblasts, suggesting that α-DG–laminin interaction in vivo is important for maintenance of the proliferative activity of satellite cells.

2. Results

2.1. Inactivation of the POMGnT1 gene in mice

We mutated the POMGnT1 gene by replacing exon 18 with a neomycin-resistance gene in mouse ES cells (depicted in Fig. 1). Two ES clones successfully entered the germline. Although there was no evidence of embryonic lethality, more than 60% of the homozygotes died within 3 weeks of birth. Survivors were smaller than their wild-type littermates (Fig. 3A) throughout life, but most of them had a normal life span. We confirmed that the POMGnT1$^{-/-}$ mice completely lacked the POMGnT1 enzyme activity (Fig. 2A). A monoclonal antibody, VIA4-1, that reacts with the suger moiety of α-DG gave no signal in either POMGnT1$^{-/-}$ brain (Fig. 2B) or muscle (data not shown). A polyclonal antibody against α-DG core protein revealed that the POMGnT1$^{-/-}$ brain expresses approximately 80 kDa α-DG protein, which is much smaller than that seen in the wild-type brain (ca. 110 kDa) (Fig. 2C). We next examined whether α-DG in POMGnT1$^{-/-}$ brain binds laminin. Wheat germ agglutinin (WGA)-enriched brain protein from control and POMGnT1$^{-/-}$ mice was separated on

SDS–PAGE gels, blotted onto a PVDF membrane, incubated with EHS laminin, and then bound laminin was detected by an anti-laminin antibody. α-DG in POMGnT1$^{-/-}$ brain failed to bind to laminin (Fig. 2D).

2.2. POMGnT1$^{-/-}$ muscle shows very mild dystrophic changes

Immunohistochemistry of cross-sections of tibialis anterior (TA) muscles showed that dystrophin and other members of the DGC complex were normally expressed at the sarcolemma of POMGnT1$^{-/-}$ muscle (Fig. 3 and Table 1). Laminin α2 chain was detected around POMGnT1$^{-/-}$ muscle fibers. On H.E.-stained cross-sections, surprisingly, the POMGnT1$^{-/-}$ muscle showed almost normal morphology. Central nucleation of myofibers indicates regeneration events in the past. In the TA muscles of 4-week-old wild-type mice, 0.25% of myofibers were centrally nucleated. In POMGnT1$^{-/-}$ mice, 0.28% of the myofibers had central nuclei. In contrast, ca. 40–50% of myofibers of age-matched mdx mice were centrally nucleated. Even at 24 months of age, the percentage of centrally nucleated myofibers was lower (3.6%) in POMGnT1$^{-/-}$ TA muscle, compared with age-matched wild-type TA muscle (9.0%). POMGnT1$^{-/-}$ TA muscle also lacked other signs of degeneration and regeneration. Electrophoresis of muscle extracts on glycerol SDS–PAGE gels showed no difference in MyHC isoform composition of quadriceps and gastrocnemius muscles between POMGnT1$^{-/-}$ and wild-type littermates (data not shown). In both wild-type and POMGnT1$^{-/-}$ muscle, the muscle basal lamina was normally formed (Supplementary Fig. 1). Electron microscopy also showed that the sarcomere structures are almost normal in POMGnT1$^{-/-}$ mice. We next examined the serum creatine kinase (CK) levels, an index of on-going muscle damage, in wild-type, POMGnT1$^{-/-}$, and age-matched mdx mice (Fig. 5). The serum CK levels of 5- to 20-week-old POMGnT1$^{-/-}$ mice were slightly higher (av. 586 U/L, n = 10) (p < 0.05) than those of wild-type littermates (less than 100 U/L, n = 4), but were much lower than those of mdx mice (more than 5000 U/L, n = 3, p < 0.01). The serum CK levels of 2-year-old POMGnT1$^{-/-}$ mice were still low (less than 300 U/L, n = 4).

2.3. Repetitive muscle injury causes more fibrosis and fatty infiltration in POMGnT1$^{-/-}$ than in WT TA muscle

Dystroglycans expressed on the cell membrane of satellite cells are proposed to play an important role in muscle regeneration (Cohn et al., 2002). In addition, the average size of POMGnT1$^{-/-}$ myofibers was smaller than those of wild-type myofibers (Fig. 4). Moreover, the number of myofibers is reduced in POMGnT1$^{-/-}$ skeletal muscle of neonatal and adult POMGnT1 mice, suggesting proliferation defect of POMGnT1$^{-/-}$ myoblasts (Fig. 4). To test the hypothesis, we damaged POMGnT1$^{-/-}$ TA muscle by cardiotoxin (CTX) and examined their regeneration. After single cardiotoxin injection, POMGnT1$^{-/-}$ muscle regenerated well like wild-type (data not shown). Next, we injected CTX into TA muscles of POMGnT1$^{-/-}$ and heterozygous littermates three times at intervals of 2 weeks, or 1 week interval, and examined the muscle. We summarized the results in Fig. 6. POMGnT1$^{-/-}$ muscle showed more fibrosis and
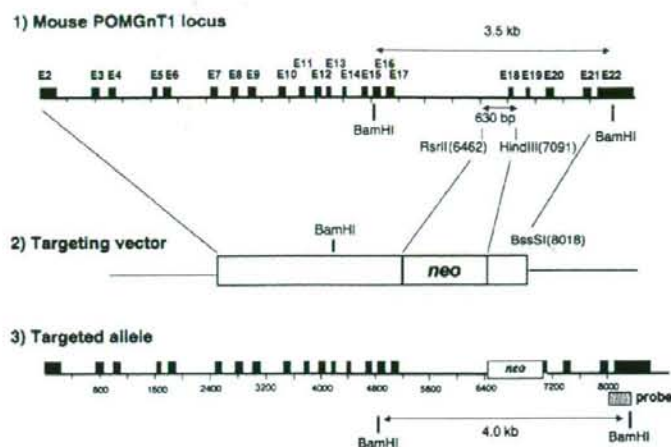
Fig. 1 – Targeted disruption of the mouse POMGnT1 gene in embryonic stem (ES) cells. The successfully targeted allele lacks a 630 bp-genome fragment containing exon 18, and instead has a neo resistance gene. Recombination in ES cells was confirmed by Southern blotting with the probe shown by a shaded box. The nucleic acid numbers are from AB053221 in GenBank.

fatty infiltration, which is a sign of inefficient muscle regeneration, than POMGnT1$^{+/-}$ muscle. Together with reduced numbers of myofibers in muscle, the results suggest that the function of satellite cells in POMGnT1$^{-/-}$ skeletal muscle is impaired.

2.4. Defective proliferative activity of POMGnT1$^{-/-}$ myoblasts

We next tested activation and proliferation of satellite cells on living myofibers isolated from wild-type and POMGnT1$^{-/-}$
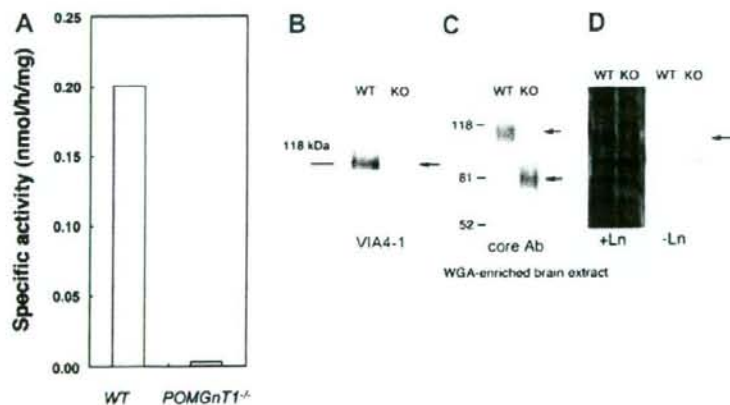

Fig. 2 – POMGnT1$^{-/-}$ mice show undetectable POMGnT1 enzyme activity and aberrant glycosylation of α-dystroglycan (α-DG) in POMGnT1$^{-/-}$ mice. (A) The amount of POMGnT1 activity is based on the amount of [^{3}H]GlcNAc transferred from UDP-GlcNAc to mannosyl peptide. The reaction product was purified by reverse-phased HPLC, and the radioactivity was measured. (B) Wheat germ agglutinin (WGA) agarose-enriched brain extracts from wild-type (WT) or POMGnT1$^{-/-}$ (KO) mice were resolved on a 7.5% SDS–PAGE gel, transferred to a PVDF membrane, and probed with anti-α-DG antibody, VIA4-1, which recognizes glycosylated α-DG. (C) The blot was incubated with polyclonal antibodies specific for α-DG core protein. The antibody detected ~110 kDa bands in wild-type brain extract, and 80 kDa bands in the brain extract of POMGnT1$^{-/-}$ mice. (D) Laminin overlay assay showing that α-DG in POMGnT1$^{-/-}$ brain does not bind laminin in vitro. +Ln, laminin was incubated with the blotted membrane. −LN, without laminin.
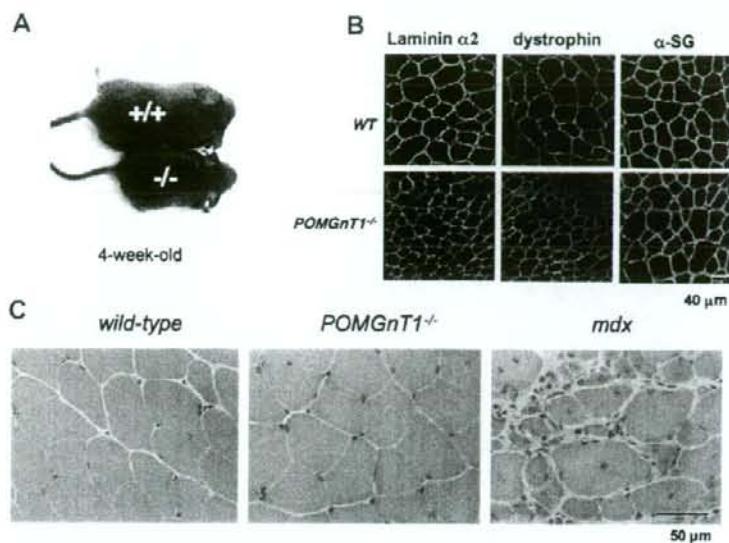
Fig. 3 – Remarkably mild dystrophic phenotypes of POMGnT1$^{-/-}$ muscle. (A) A photo of representative 4-week-old wild-type (+/+) and POMGnT1$^{-/-}$ (−/−) mice. POMGnT1$^{-/-}$ mice are smaller than wild-type littermates. (B) Immunohistochemistry of wild-type (+/+) and POMGnT1-knockout (−/−). Laminin α2 chain, dystrophin, and α-sarcoglycan are expressed normally on the sarcolemma of POMGnT1$^{-/-}$ muscle. (C) Representative H.E. staining of cross-sections of the TA muscles from POMGnT1$^{-/-}$, wild-type, and age-matched dystrophin-deficient mdx mice. POMGnT1$^{-/-}$ muscle shows minimal signs of degeneration and regeneration.

Table 1 – Summary of immunohistochemistry of hindlimb muscles of wild-type (WT) POMGnT1$^{-/-}$, and mdx mice.

	WT	POMGnT1$^{-/-}$	mdx
Laminin α2 chain	+	+	+
Dystrophin	+	+	−
α-Dystroglycan (VIA4-1)	+	−	±
Dystroglycan (core protein)	+	+	±
β-Dystroglycan	+	+	±
α-Sarcoglycan	+	+	±
α-Syntrophin	+	+	±
nNOS	+	+	±
Aquaporin 4	+	+	±
Integrin α7	+	+	++
Integrin β1	+	+	++

+, expressed; −, absent; ±, down-regulated; ++, up-regulated.

mice (Fig. 7). Three days after plating of single myofibers on Matrigel-coated 24-well plates in growth medium, the numbers of detached satellite cells (activated and proliferating satellite cells) were counted. In both extensor digitorum longus (EDL) (fast twitch muscle) and soleus (slow twitch muscle) muscles, the numbers of activated satellite cells and proliferating satellite cells (myoblasts) around the parental myofiber were more numerous in wild-type than in POMGnT1$^{-/-}$ (Fig. 7). Furthermore, wild-type satellite cells migrate a little faster than POMGnT1$^{-/-}$ satellite cells on transwells (data not shown), although the difference was little. Therefore, our results suggest that POMGnT1$^{-/-}$ satellite cells are activated more slowly or proliferate more slowly than wild-type. We next isolated satellite cells from hind limb muscles of wild-type and POMGnT1$^{-/-}$ mice by a monoclonal antibody, SM/C-2.6, and flow cytometry (Fukada et al., 2007), and examined their proliferation rate. The total yield of satellite cells per gram of POMGnT1$^{-/-}$ muscle tissue was nearly the same as those of wild-type muscle (data not shown). The percentage of Ki67-positive satellite cells (cycling cells) was less than 1% in both wild-type and POMGnT1$^{-/-}$ mice, indicating that they are in the quiescent stage (data not shown). However, after plating wild-type and POMGnT1$^{-/-}$ satellite cells onto Matrigel-coated 6-well plates at the same density, we found that POMGnT1$^{-/-}$ satellite cells grew poorly in growth medium (Fig. 7B). The timing of activation (i.e. enlargement of the cytoplasm and MyoD expression) was the same with that of wild-type satellite cells (data not shown). Next, we cultured satellite cells on Matrigel-coated 24-well-plates in growth medium, and the cells growth was evaluated by MTT assay 1, 2, 3, 4, 5, 6, and 7 days after plating (Fig. 8). The assay revealed that wild-type myoblasts proliferated more rapidly than POMGnT1$^{-/-}$ myoblasts in vitro. POMGnT1$^{-/-}$ myoblasts fused normally to form multinucleated myotubes in differentiation conditions like the wild-type (data not shown), and there was no significant difference in the fusion index between wild-type (45%) and POMGnT1$^{-/-}$ myoblasts (40%) ($p > 0.05$).
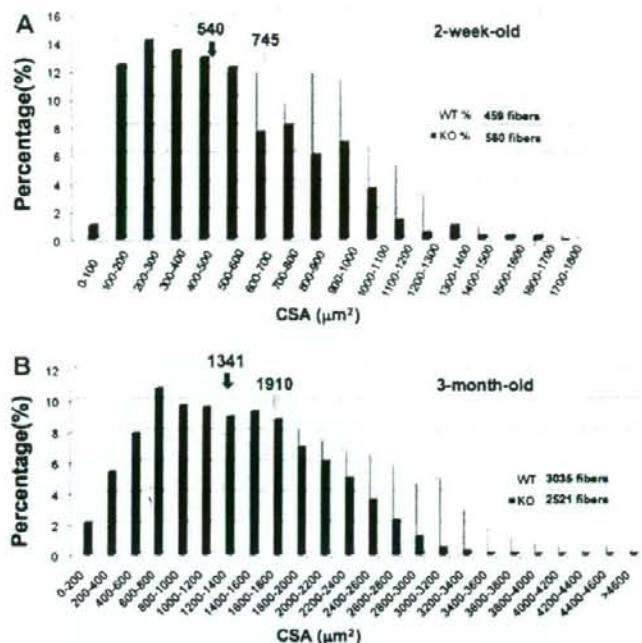
Fig. 4 – Cross-sectional area (CSA) of myofibers of POMGnT1$^{-/-}$ and wild-type mice. (A) A representative frequency graph of CSA of rectus femoris muscles from 2-week-old POMGnT1$^{-/-}$ (blue) and wild-type (light blue) littermates. The cross-sections were stained with anti-laminin α2 chain antibody. CSA of 459 POMGnT1$^{-/-}$ fibers and 580 wild-type fibers were measured and plotted. X-axis indicates CSA (μm²), and Y-axis indicates percentages. Arrows indicate the averages. The total number of myofibers was also reduced in POMGnT1$^{-/-}$ mice (4169 vs. 3510). (B) The CSA of myofibers in TA muscles from 3-month-old POMGnT1$^{-/-}$ (blue) and wild-type (light blue) male mice was plotted as in (A)). In (B), almost all myofibers were measured (3035 fibers in wild-type TA and 2521 fibers in POMGnT1$^{-/-}$ TA).
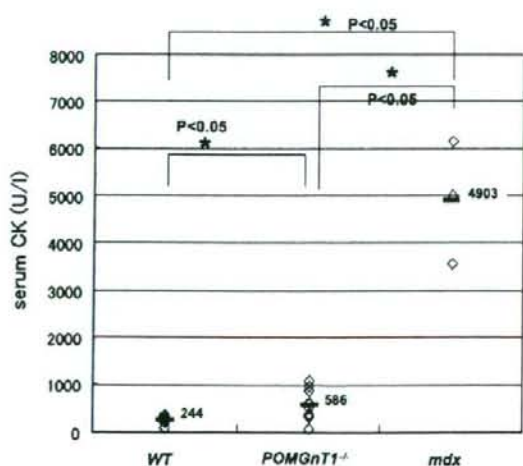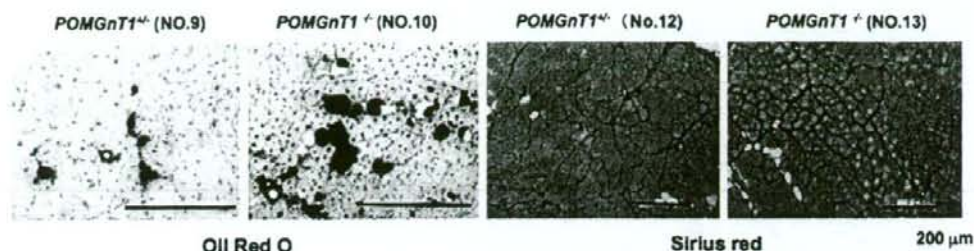

Fig. 5 – Serum CK levels of POMGnT1$^{-/-}$, wild-type, and mdx mice. Serum CK levels of 7–20 weeks old POMGnT1$^{-/-}$ mice (5 males and 5 females), wild-type littermates (3 males and 1 female), and three male mdx mice were measured and plotted on the graph with average. *p < 0.05.

Next, we examined whether restoration of the expression of the POMGnT1 gene in mutant myoblasts improved their proliferation. To this end, we prepared a retrovirus vector, (pMX-POMGnT1-IRES-GFP) expressing human POMGnT1 and GFP. The recombinant retrovirus successfully restored O-mannosyl glycosylation of α-DG (Fig. 7A), but the proliferation rate was not changed (Fig. 8B).

2.5.   Cell growth signaling in POMGnT1$^{-/-}$ myoblasts

It was previously reported that enhanced expression of α7β1 integrin ameliorates the development of muscular dystrophy and extends longevity in α7BX2-mdx/utr($^{-/-}$) transgenic mice (Burkin et al., 2001; Burkin et al., 2005), suggesting that integrin compensates for the function of α-DG in skeletal muscle to some extent. Therefore, we next examined the expression of β1-integrin in wild-type and POMGnT1$^{-/-}$ myoblasts (Supplementary Fig. 1). Western blotting, however, showed no difference between the β1-integrin protein levels in wild-type and POMGnT1$^{-/-}$ myoblasts (Supplementary Fig. 1A). Furthermore, FACS analysis showed similar levels of β1 integrin expression on the surfaces of myoblasts (Supplementary Fig. 1B). We then examined the activation levels of Akt and GSK-3β, both of which are involved in the

POMGnT1⁺ᐟ⁻ (NO.9)   **POMGnT1⁻ᐟ⁻ (NO.10)**   **POMGnT1⁺ᐟ⁻ (No.12)**   **POMGnT1⁻ᐟ⁻ (NO.13)**

Oil Red O   Sirius red   200 µm

	genotype	sex	age	CTX interval(x3)	Fatty infiltration	Fibrosis
1	+/-	F	3M	2w	-	-
2	+/-	F	3M	2w	-	-
3	+/-	F	3M	2w	- -+	- -+
4	+/-	F	3M	2w	+	- -+
5	-/-	M	3M	2w	+	- -+
6	-/-	F	3M	2w	++	- -+
7	+/-	F	11M	1w	+	+
8	-/-	F	8.5M	1w	+	++
9	+/-	F	8.5M	1w	+	- -+
10	-/-	F	8.5M	1w	+ -++	+ -++
11	+/-	M	8.5M	1w	+	+
12	+/-	M	8.5M	1w	++	+
13	-/-	M	8.5M	1w	++	++

Fig. 6 – Impaired muscle regeneration of POMGnT1⁻ᐟ⁻ mice. upper panel: representative Oil red O-stained or Sirius red-stained cross-sections of TA muscles of POMGnT1⁻ᐟ⁻ (-/-) and POMGnT1⁺ᐟ⁻ (+/-) mice after three rounds of degeneration/regeneration evoked by cardiotoxin injection. One week after the last CTX injection, TA muscles were dissected, sectioned by a cryostat, fixed, and stained. lower table: Summary of fatty infiltration and fibrosis in regenerated muscles. CTX was injected into TA muscles three times with 2 weeks interval (2w) or 1 week interval (1w). The age at the first injection was shown. (-), well regenerated with minimal changes. (- -+), sporadic fatty regeneration or slight fibrosis between fibers. (+), mild fatty infiltration or mild fibrosis. (++), dense fatty infiltration or extensive fibrosis. F, female; M, male.

regulation of cell survival and proliferation. The levels of phosphorylation of these two kinases in POMGnT1⁻ᐟ⁻ myoblasts were similar with those in wild-type myoblasts (Supplementary Fig. 1C). Consistent with these observations, TUNEL assay indicated that apoptosis is rare both in POMGnT1⁻ᐟ⁻ and wild-type muscles (data not shown).

3.   Discussion

In this study, we showed that in spite of mild muscle degeneration, the POMGnT1⁻ᐟ⁻ satellite cells have much lower proliferative activity than wild-type satellite cells. The defect was not recovered by restoration of normal glycosylation of α-DG in mutant satellite cells. Together with the reduced sizes and the reduced numbers of myofibers of neonatal and adult POMGnT1⁻ᐟ⁻ mice, these observations suggest that deficiency of POMGnT1 enzymatic activity impairs the functions of satellite cells.

3.1.   Two mouse models of muscle–eye–brain (MEB) disease

Our POMGnT1⁻ᐟ⁻ mice are the second mouse model of MEB disease. The first one was generated by gene trapping with a retroviral vector inserted into the second exon of the mouse POMGnT1 locus (Liu et al., 2006). As described in the literature, the phenotype is similar to ours with some

differences. Our model shows much milder muscle phenotypes than the previously reported model, but also shows much a lower survival rate in the postnatal stage than the first model does. This would be due to more severe developmental abnormalities of the central nervous system of our mouse model, including disruption of the glia limitans, abnormal migration of neurons, and reactive gliosis in the cerebral cortex (manuscript in preparation), although these are also observed in the first model (Yang et al., 2007; Hu et al., 2007).

Mutation of the POMGnT1 gene is the cause of muscle–eye–brain disease (MEB) (Yoshida et al., 2001), which is characterized by severe congenital muscular dystrophy (Voit and Tome, 2004). Although glycosylation of α-DG was completely perturbed in our model, the POMGnT1⁻ᐟ⁻ muscle showed only marginal pathological changes. Furthermore, POMGnT1⁻ᐟ⁻ muscle showed normally formed muscle basal lamina on EM. These observations are in sharp contrast to the condition in humans. One possibility is that in the mouse, molecules other than α-DG are involved in the linkage of the sarcolemma with the extracellular matrix proteins, stabilizing the plasma membrane. As a candidate molecule, we examined β1-integrin expression in POMGnT1⁻ᐟ⁻ muscle, but found that the level was not up-regulated. Therefore, the mechanism that explains this discrepancy remains to be clarified in a future study.
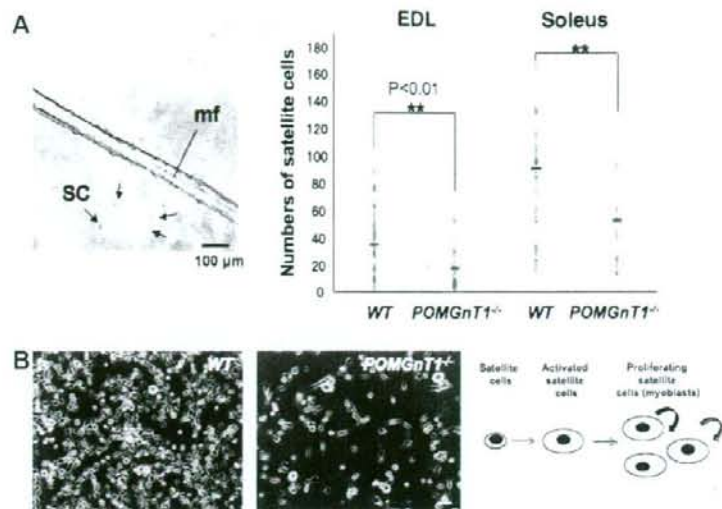
Fig. 7 – Activation and proliferation of satellite cells from WT and POMGnT1$^{-/-}$ mice. (A) Isolated myofibers were plated on Matrigel-coated 24 well-plates at one myofiber per well. Three days later, activated satellite cells (SC, arrows) around the parental fiber (mf) were counted and plotted. Small horizontal bars indicate the average number of activated/proliferating satellite cells originating from a myofiber from three independent experiments. Student's t-test. $^{**}p < 0.01$ (wild-type vs. POMGnT1$^{-/-}$ mice). (B) Satellite cells from WT and POMGnT1$^{-/-}$ mice 7 days after plating onto Matrigel-coated 24-well-plates at 2.5×10^3 cells/well. Scale bar, 100 μm.
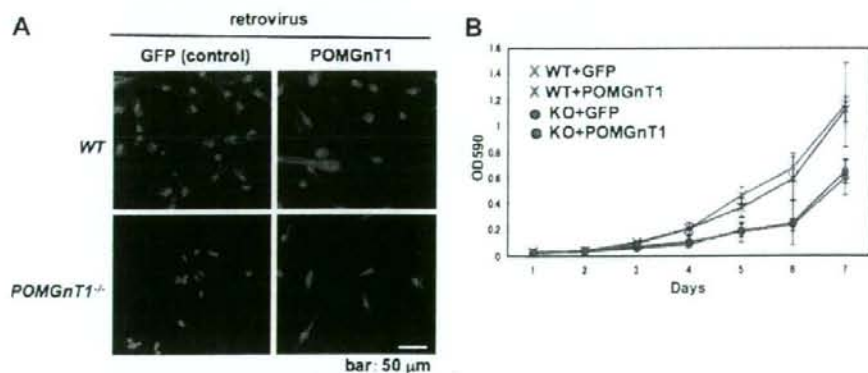

Fig. 8 – Restoration of POMGnT1 expression in POMGnT1$^{-/-}$ myoblasts does not improve proliferation of cells. (A) Wild-type (WT) and POMGnT1$^{-/-}$ myoblasts were transduced with a retrovirus expressing both POMGnT1 and GFP (POMGnT1) or only GFP (GFP, control), and the FACS-purified transduced cells were stained with anti-glycosylated α-DG monoclonal antibody (VIA4-1; red) and DAPI (Nucleus, blue). Note that the glycosylation of α-DG in POMGnT1$^{-/-}$ myoblasts was completely recovered by a retrovirus vector expressing POMGnT1. (B) MTT assay of wild-type (WT) and POMGnT1$^{-/-}$ myoblasts after infection with retrovirus vectors. Impaired proliferation of POMGnT1$^{-/-}$ myoblasts was not recovered by retrovirus-mediated expression of POMGnT1. Representative data of three independent experiments are shown.

3.2. Null mutation in POMGnT1 reduces proliferative activity of muscle satellite cells

POMGnT1$^{-/-}$ myoblasts proliferate poorly in vitro. This observation suggested that the proliferation of myoblasts is stimulated by growth signals via laminin-α-DG interaction.

However, retrovirus vector-mediated gene transfer of the POMGnT1 gene, which successfully restored O-mannosyl glycosylation of α-DG, did not restore the proliferation activity of the POMGnT1$^{-/-}$ myoblasts. DMD myoblasts proliferate poorly and quickly reach senescence. The impaired proliferation activity has been ascribed to repeated activation of

satellite cells due to repetitive cycles of muscle degeneration and regeneration (Blau et al., 1983). In contrast, POMGnT1$^{-/-}$ muscle lacks signs of active regeneration. Therefore, the reduced proliferation activity of POMGnT1$^{-/-}$ mouse myoblasts is not likely due to excessive cell division of satellite cells. Rather, it is likely that α-DG-laminin interaction in the niche, i.e. beneath the basal lamina of skeletal muscle myofibers, is important for maintenance of proliferative activity of satellite cells. However, the possibility that POMGnT1-deficiency causes aberrant glycosylation of molecules other than α-DG should be also tested.

Our results also suggested that the lack of α-DG-laminin interaction resulted in reduced numbers of muscle fibers (hypoplasia). Importantly, we found that myofibers of older POMGnT1$^{-/-}$ mice tend to be hypertrophied (Supplementary Fig. 2). POMGnT1$^{-/-}$ muscle might compensate the muscle power by hypertrophy of the myofibers. This is consistent with our observation that POMGnT1$^{-/-}$ muscle increases its mass in an overload model (unpublished data). Importantly, recent studies suggest that this process is satellite cell-independent (Sandri M., 2008).

Recently, Liu et al. showed that over-expression of integrin α7β1 in C2C12 myoblasts promoted proliferation of the cells (Liu et al., 2008). Importantly, however, we did not observe up-regulation of integrin α7β1 expression in POMGnT1$^{-/-}$ satellite cells. These observations suggest that dystroglycans and integrins have distinct roles in the regulation of muscle satellite cells.

In summary, we generated POMGnT1-null mice. The mice showed low serum creatine kinase levels and minimal signs of muscle degeneration and regeneration. Nonetheless, POMGnT1$^{-/-}$ muscle showed the reduction in the size and the number of myofibers. Furthermore, repeated injection of cardiotoxin showed impaired muscle regeneration in POMGnT1$^{-/-}$ mice. POMGnT1$^{-/-}$ myoblasts proliferated poorly in vitro. Over-expression of protein restored glycosylation of α-DG, but did not improve the proliferation of POMGnT1$^{-/-}$ myoblasts at all. Collectively, our results suggest that POMGnT1 enzymatic activity is important for maintenance of the proliferative activity of satellite cells in vivo.

4.   Experimental procedures

4.1.   Generation of POMGnT1$^{-/-}$ mice

The targeting strategy in ES cells is depicted in Fig. 1. Genomic DNA (8.6 kb) covering almost the entire POMGnT1 gene was isolated from 129/SvJ mice by using two specific primers: m1F2 primer, 5′-gat tcc tga agt cat gga ctg gc-3′ and m1B5, 5′-tct aaa ggt ctc tgt gtg agt ctg tca g-3′. The PCR product was then cloned into a TOPO TA cloning vector (Invitrogen, Carlsbad, CA) and sequenced (AB053221). To construct the targeting vector, a 630-bp RsrII-Hind III fragment, containing exon18 was replaced with a neo expression cassette (Stratagene) (Fig. 1). Electroporation and screening of ES cells (129Svev origin) were performed by Ingenious Targeting Laboratory, Inc. (Stony Brook, NY). Homologous recombination in ES cells was confirmed by Southern blotting. Two independent positive ES clones were injected into C57BL/6 blastocysts,

which gave rise to offspring carrying the mutated allele. Genotyping of the mice was done by PCR. One primer set is designed to amplify exon 18: F2, 5′-cag cag ttt cct tcc ttc taa ccc-3′ and B4, 5′-att tgg tct ggt ccc ttg gct c-3′ (278 bp). Neo primers were used to amplify the neo resistance gene, and thereby detect the mutant allele: neo-F, 5′-agg cta ttc ggc tat gac tgg g-3′, and neo-R, 5′-tac ttt ctc ggc agg agc aag gtg-3′ (288 bp). Dystrophin-deficient mdx mice of C57BL/6 genetic background were provided by T. Sasaoka at the National Institute for Basic Biology, Japan. The Experimental Animal Care and Use Committee of the National Institute of Neuroscience approved all experimental protocols.

4.2.   POMGnT1 enzymatic activity

Brains were obtained from 8-week-old mice and homogenized with nine volumes (weight/volume) of 10 mM Tris-HCl, pH 7.4, 1 mM EDTA, and 250 mM sucrose. After centrifugation at 900g for 10 min, the supernatant was subjected to ultracentrifugation at 100,000g for 1 h. The precipitates were used as the microsomal membrane fraction. The protein concentration was determined by BCA assay (Pierce, Rockford, IL). The enzymatic activity assay measured the amount of [^{3}H]GlcNAc transferred to a mannosyl peptide (Akasaka-Manya et al., 2004). Briefly, a reaction mixture containing 140 mM Mes buffer (pH 7.0), 1 mM UDP-[^{3}H]GlcNAc (80,000 dpm/nmol, PerkinElmer, Inc., Wellesley, MA), 2 mM mannosyl peptide (Ac-Ala-Ala-Pro-Thr-(Man)-Pro-Val-Ala-Ala-Pro-NH$_2$), 10 mM MnCl$_2$, 2% Triton X-100, 5 mM AMP, 200 mM GlcNAc, 10% glycerol, and 100 μg of microsomal membrane fraction was incubated at 37 °C for 1 h. After boiling for 3 min, the mixture was analyzed by reverse phase HPLC using a Wakopak 5C18-200 column (4.6 × 250 mm, Wako Pure Chemical Industries, Osaka, Japan). The gradient solvents were aqueous 0.1% trifluoroacetic acid (solvent A) and acetonitrile containing 0.1% trifluoroacetic acid (solvent B). The mobile phase consisted of 100% A for 10 min and then a linear gradient to 75% A:25% B over 25 min. Peptide separation was monitored at 214 nm, and the radioactivity of each fraction (1 ml) was measured using a liquid scintillation counter.

4.3.   Antibodies

All antibodies used in Western blotting, immunohistochemistry, and FACS are listed in Supplementary Table 1.

4.4.   Histology and immunohistochemical analysis

Muscle cryosections (6–10 μm) were stained with hematoxylin and eosin (H&E), or treated with 0.1% Triton X-100, blocked with 5% goat serum/1% BSA in PBS, then incubated with primary antibodies (Supplementary Table 1) at 4 °C overnight. After washing with PBS, specimens were incubated with a secondary antibody labeled with Alexa Fluor 488 or Alexa Fluor 568 (1:200–400 dilution; Molecular Probes) at RT for 1 h, counterstained with TOTO-3 (1:5000; Molecular Probes), and then mounted in Vectashield (Vector). The images were recorded using a confocal laser scanning microscope system TCSSP* (Leica). For fiber size measurement, cross-sections of muscle were stained with anti-laminin α2

antibody and recorded and quantified by a digital microscope, BIOREVO (http://www.biorevo.jp; KEYENCE, Osaka, Japan).

4.5. Western blotting

Western blotting was performed as previously described (Hosaka et al., 2002). In brief, 20 μg of muscle proteins were separated on 7.5% SDS–PAGE gels and transferred to a PVDF membrane (Millipore, Bedford, MA). After incubation with primary antibodies (Supplementary Table 1), the membranes were incubated in HRP-labeled secondary antibodies (1:5000 dilution) (Amersham Biosciences, UK). The signals were detected by using an ECL plus Western Blotting Detection System (GE Healthcare, Buckinghamshire, UK).

4.6. Laminin blot overlay assay

An overlay assay was performed as described by Moore et al. (2002). In brief, WGA-enriched homogenates were prepared from wild-type and POMGnT1$^{-/-}$ brains, separated on SDS–PAGE gels, blotted onto a PDVF membrane, and incubated with mouse EHS laminin (Trevigen, Gaithersburg, MD, USA). Bound laminin was probed with anti-laminin antibody (Sigma, St. Louis, MO) and ECL system (GE Healthcare, Buckinghamshire, UK).

4.7. Single fiber preparation and culture

Single fibers were prepared from extensor digitorum longus (EDL) and soleus muscles of wild-type and POMGnT1$^{-/-}$ mice as described by Rosenblatt et al. (1995). Each fiber was plated onto Matrigel (BD Biosciences, Bedford, MA)-coated 24-well plates and cultured in growth medium for 3 days. Then, the number of cells around the parental fiber was counted.

4.8. Isolation of satellite cells, proliferation assay, and fusion index

Satellite cells were prepared from wild-type and POMGnT1$^{-/-}$ mice by FACS as previously described (Fukada et al., 2007). Sorted cells were plated on Matrigel-coated 24-well-plates at a density of 1×10^4 cells/well in a growth medium, DMEM (High glucose; Wako, Osaka), supplemented with 20% fetal bovine serum (Equitech-bio, Inc., Kerville, TX), human recombinant bFGF (2.5 ng/ml) (Invitrogen), recombinant mouse HGF (25 ng/ml) (R&D Systems, Minneapolis, MN), and heparin (5 μg/ml) (Sigma). For the MTT assay, 100 μl of 0.5% MTT (3-(4,5-dimethylthiazol-2-yl)-2,5-diphenyltetrazolium bromide) (Dojindo, Kumamoto, Japan) was added to the culture at each time point, and after 4 h incubation, the cells were collected in 1 ml of acid isopropanol solution. OD_{590} was measured and plotted. After reaching 70% confluency, the cells were induced to differentiate into myotubes by low-serum medium (5% horse serum/DMEM), and 18 h later, the cells were fixed, stained with anti-sarcomeric α-actinin antibody and DAPI (nuclei). Fusion index was calculated as (the numbers of nuclei in the myotubes/total nuclei) × 100%.

4.9. Production of retrovirus vectors

pMXs-IG (Kitamura et al., 2003) was kindly provided by T.Kitamura at Tokyo University. Human POMGnT1 cDNA, which has an Xpress epitope and a His-tag at the N-terminal (Akasaka-Manya et al., 2004), was cloned into the multi-cloning site upstream of IRES-GFP of the vector. Vector particles were produced by transfection of the vector plasmid into PLAT-E packaging cells (Kitamura et al., 2003). Proliferating satellite cells (myoblasts) were incubated with the viral vectors overnight and 4 days later, successfully transduced GFP-positive cells were collected by FACS, and the proliferation rate was evaluated by MTT assay.

4.10. Electron microscopy

Mice were perfused transcardially with a solution of 2% paraformaldehyde and 2.5% glutaraldehyde in PBS under deep pentobarbital anesthesia. The anterior tibial muscles were excised, embedded in 3% agarose, and sections (70 μm in thickness) were prepared on a Vibratome. Sections were fixed in OsO$_4$, ehydrated, and embedded in Cartepoxy resin. Ultrathin sections were prepared, stained with lead citrate and uranyl acetate, and observed under a Hitachi H-7000 transmission electron microscope.

4.11. Measurement of serum creatine kinase (CK)

Blood samples were obtained from the tail vein or directly from the heart at sacrifice. Serum CK level was measured by colorimetric assay using an FDC3500 clinical biochemistry autoanalyzer (FujiFilm Medical Co., Tokyo, Japan).

4.12. Cardiotoxin (CTX) injection

To induce muscle regeneration, CTX (10 μmol/L in saline; Sigma, St. Louis, MO) was injected into the tibialis anterior (TA) muscles three times at indicated intervals. The muscle cross-sections were stained with Oil red O (Muto Pure Chemicals Co., Ltd., Tokyo, Japan) to detect lipid droplets, or with Sirius red F3B (Sigma Chemical Co., St. Louis, MO) in saturated picric acid to stain collagen fibers.

Appendix A. Supplementary data

Supplementary data associated with this article can be found, in the online version, at doi:10.1016/j.mod.2008.12.001.

REFERENCES

Akasaka-Manya, K., Manya, H., Kobayashi, K., Toda, T., Endo, T., 2004. Structure–function analysis of human protein O-linked mannose beta1,2-N-acetylglucosaminyltransferase 1, POMGnT1. Biochem. Biophys. Res. Commun. 320, 39–44.

Blau, H.M., Webster, C., Pavlath, G.K., 1983. Defective myoblasts identified in Duchenne muscular dystrophy. Proc. Natl. Acad. Sci. USA 80, 4856–4860.

Burkin, D.J., Wallace, G.Q., Milner, D.J., Chaney, E.J., Mulligan, J.A., Kaufman, S.J., 2005. Transgenic expression of α7β1 integrin maintains muscle integrity, increases regenerative capacity, promotes hypertrophy, and reduces cardiomyopathy in dystrophic mice. Am. J. Pathol. 166, 253–263.

Burkin, D.J., Wallace, G.Q., Nicol, K.J., Kaufman, D.J., Kaufman, S.J., 2001. Enhanced expression of the alpha 7 beta 1 integrin reduces muscular dystrophy and restores viability in dystrophic mice. J. Cell Biol. 152, 1207–1218.

Campanelli, J.T., Roberds, S.L., Campbell, K.P., Scheller, R.H., 1994. A role for dystrophin-associated glycoproteins and utrophin in agrin-induced AChR clustering. Cell 77, 663–674.

Cohn, R.D., Henry, M.D., Michele, D.E., Barresi, R., Saito, F., Moore, S.A., Flanagan, J.D., Skwarchuk, M.W., Robbins, M.E., Mendell, J.R., Williamson, R.A., Campbell, K.P., 2002. Disruption of DAG1 in differentiated skeletal muscle reveals a role for dystroglycan in muscle regeneration. Cell 110, 639–648.

Endo, T., Toda, T., 2003. Glycosylation in congenital muscular dystrophies. Biol. Pharm. Bull. 26, 1641–1647.

Fukada, S., Uezumi, A., Ikemoto, M., Masuda, S., Segawa, M., Tanimura, N., Yamamoto, H., Miyagoe-Suzuki, Y., Takeda, S., 2007. Molecular signature of quiescent satellite cells in adult skeletal muscle. Stem Cells 25, 2448–2459.

Gee, S.H., Montanaro, F., Lindenbaum, M.H., Carbonetto, S., 1994. Dystroglycan-alpha, a dystrophin-associated glycoprotein, is a functional agrin receptor. Cell 77, 675–686.

Hosaka, Y., Yokota, T., Miyagoe-Suzuki, Y., Yuasa, K., Imamura, M., Matsuda, R., Ikemoto, T., Kameya, S., Takeda, S., 2002. Alpha1-syntrophin-deficient skeletal muscle exhibits hypertrophy and aberrant formation of neuromuscular junctions during regeneration. J. Cell Biol. 158, 1097–1107.

Hu, H., Yang, Y., Eade, A., Xiong, Y., Qi, Y., 2007. Breaches of the pial basement membrane and disappearance of the glia limitans during development underlie the cortical lamination defect in the mouse model of muscle–eye–brain disease. J. Comp. Neurol. 502, 168–183.

Ibraghimov-Beskrovnaya, O., Ervasti, J.M., Leveille, C.J., Slaughter, C.A., Sernett, S.W., Campbell, K.P., 1992. Primary structure of dystrophin-associated glycoproteins linking dystrophin to the extracellular matrix. Nature 355, 696–702.

Kanagawa, M., Michele, D.E., Satz, J.S., Barresi, R., Kusano, H., Sasaki, T., Timpl, R., Henry, M.D., Campbell, K.P., 2005. Disruption of perlecan binding and matrix assembly by post-translational or genetic disruption of dystroglycan function. FEBS Lett. 579, 4792–4796.

Kanagawa, M., Toda, T., 2006. The genetic and molecular basis of muscular dystrophy: roles of cell–matrix linkage in the pathogenesis. J. Hum. Genet. 51, 915–926.

Kitamura, T., Koshino, Y., Shibata, F., Oki, T., Nakajima, H., Nosaka, T., Kumagai, H., 2003. Retrovirus-mediated gene transfer and expression cloning: powerful tools in functional genomics. Exp. Hematol. 31, 1007–1014.

Liu, J., Ball, S.L., Yang, Y., Mei, P., Zhang, L., Shi, H., Kaminski, H.J., Lemmon, V.P., Hu, H., 2006. A genetic model for muscle–eye–brain disease in mice lacking protein O-mannose 1,2-N-acetylglucosaminyltransferase (POMGnT1). Mech. Dev. 123, 228–240.

Liu, J., Burkin, D.J., Kaufman, S.J., 2008. Increasing alpha 7 beta 1-integrin promotes muscle cell proliferation, adhesion, and resistance to apoptosis without changing gene expression. Am. J. Physiol. Cell Physiol. 294, C627–C640.

Michele, D.E., Barresi, R., Kanagawa, M., Saito, F., Cohn, R.D., Satz, J.S., Dollar, J., Nishino, I., Kelley, R.I., Somer, H., Straub, V., Mathews, K.D., Moore, S.A., Campbell, K.P., 2002. Post-translational disruption of dystroglycan–ligand interactions in congenital muscular dystrophies. Nature 418, 417–422.

Moore, S.A., Saito, F., Chen, J., Michele, D.E., Henry, M.D., Messing, A., Cohn, R.D., Ross-Barta, S.E., Westra, S., Williamson, R.A., Hoshi, T., Campbell, K.P., 2002. Deletion of brain dystroglycan recapitulates aspects of congenital muscular dystrophy. Nature 418, 422–425.

Peng, H.B., Ali, A.A., Daggett, D.F., Rauvala, H., Hassell, J.R., Smalheiser, N.R., 1998. The relationship between perlecan and dystroglycan and its implication in the formation of the neuromuscular junction. Cell Adhes. Commun. 5, 475–89.

Rosenblatt, J.D., Lunt, A.I., Parry, D.J., Partridge, T.A., 1995. Culturing satellite cells from living single muscle fiber explants. In Vitro Cell Dev. Biol. Anim. 31, 773–779.

Sandri M., 2008. Signaling in muscle atrophy and hypertrophy. Physiology (Bethesda) 23, 160–170.

Sugita, S., Saito, F., Tang, J., Satz, J., Campbell, K., Südhof, T.C., 2001. A stoichiometric complex of neurexins and dystroglycan in brain. J. Cell Biol. 154, 435–445.

Voit, T., Tome, F.S., 2004. The congenital muscular dystrophies. In: Engel, A.G., Franzini-Armstrong, C. (Eds.), Myology. McGraw-Hill, New York, pp. 1203–1238.

Yang, Y., Zhang, P., Xiong, Y., Li, X., Qi, Y., Hu, H., 2007. Ectopia of meningeal fibroblasts and reactive gliosis in the cerebral cortex of the mouse model of muscle–eye–brain disease. J. Comp. Neurol. 505, 459–477.

Yoshida, A., Kobayashi, K., Manya, H., Taniguchi, K., Kano, H., Mizuno, M., Inazu, T., Mitsuhashi, H., Takahashi, S., Takeuchi, M., Herrmann, R., Straub, V., Talim, B., Voit, T., Topaloglu, H., Toda, T., Endo, T., 2001. Muscular dystrophy and neuronal migration disorder caused by mutations in a glycosyltransferase, POMGnT1. Dev. Cell 1, 717–724.

Generation of transplantable, functional satellite-like cells from mouse embryonic stem cells

Hsi Chang,* Momoko Yoshimoto,*,† Katsutsugu Umeda,* Toru Iwasa,* Yuta Mizuno,* So-ichiro Fukada,‡ Hiroshi Yamamoto,‡ Norio Motohashi,§ Yuko-Miyagoe-Suzuki,§ Shin'ichi Takeda,§ Toshio Heike,*,[1] and Tatsutoshi Nakahata*

*Department of Pediatrics, Kyoto University Graduate School of Medicine, Kyoto, Japan; †Indiana University School of Medicine Wells Center for Pediatric Research, Indianapolis, Indiana, USA; ‡Department of Immunology, Graduate School of Pharmaceutical Science, Osaka University, Osaka, Japan; and §Department of Molecular Therapy, National Institution of Neuroscience, National Center of Neurology and Psychiatry, Tokyo, Japan

ABSTRACT   Satellite cells are myogenic stem cells responsible for the postnatal regeneration of skeletal muscle. Here we report the successful *in vitro* induction of Pax7-positive satellite-like cells from mouse embryonic stem (mES) cells. Embryoid bodies were generated from mES cells and cultured on Matrigel-coated dishes with Dulbecco's modified Eagle medium containing fetal bovine serum and horse serum. Pax7-positive satellite-like cells were enriched by fluorescence-activated cell sorting using a novel anti-satellite cell antibody, SM/C-2.6. SM/C-2.6-positive cells efficiently differentiate into skeletal muscle fibers both *in vitro* and *in vivo*. Furthermore, the cells demonstrate satellite cell characteristics such as extensive self-renewal capacity in subsequent muscle injury model, long-term engraftment up to 24 wk, and the ability to be secondarily transplanted with remarkably high engraftment efficiency compared to myoblast transplantation. This is the first report of transplantable, functional satellite-like cells derived from mES cells and will provide a foundation for new therapies for degenerative muscle disorders.—Chang, H., Yoshimoto, M., Umeda, K., Iwasa, T., Mizuno, Y., Fukada, S., Yamamoto, H., Motohashi, N., Yuko-Miyagoe-Suzuki, Takeda, S., Heike, T., Nakahata, T. Generation of transplantable, functional satellite-like cells from mouse embryonic stem cells. *FASEB J.* 23, 000–000 (2009)

Key Words: long-term engraftment · secondary transplantation · high engraftment efficiency · self-renewal

DUCHENNE MUSCULAR DYSTROPHY (DMD; ref. 1) is a progressive, lethal muscular disorder (2) with no effective cure despite extensive research efforts. DMD results from mutations in the X-linked *dystrophin* gene (3). Dystrophin and its associated proteins function to link the intracellular actin cytoskeleton of muscle fibers to laminin in the extracellular matrix (4), thereby protecting myofibers from contraction-induced damage (5). Skeletal muscle fibers are continuously regenerated following exercise and injuries when satellite cells (6) are induced to differentiate into myoblasts that

form myotubes and replace the damaged myofibers (7, 8). This muscular regeneration is observed at a much higher frequency in DMD patients (9). Continuous damage to myofibers and constant activation of resident satellite cells due to loss of dystrophin leads to the exhaustion of the satellite cells (10, 11), and the eventual depletion of satellite cells is primarily responsible for the onset of DMD symptoms.

Successful transplantation of normal satellite cells into the skeletal muscle of DMD patients may enable *in situ* production of normal muscle tissue and create a treatment option for this otherwise fatal disease. A recent report has shown that the transplantation of satellite cells collected from mouse muscle tissues can produce muscle fibers with normal dystrophin expression in mdx mice (12–14), a model mouse for DMD (15). This study suggests that stem cell transplantation may be a viable therapeutic approach for the treatment of DMD (16).

Satellite cells are monopotent stem cells that have the ability to self-renew and to differentiate into myoblasts and myotubes to maintain the integrity of skeletal muscle (17). Satellite cells lie dormant beneath the basal lamina and express transcription factors such as Pax3 (13, 18) and Pax7 (19). Pax7, a paired box transcription factor, is particularly important for satellite cell function. A recent study of *Pax7-null* mice revealed that Pax7 is essential for satellite cell formation (19) and that the *Pax7-null* mice exhibit a severe deficiency in muscle fibers at birth and premature mortality with complete depletion of the satellite cells. Surface markers such as M-cadherin and c-met (20) are also expressed by satellite cells. However, these markers are not specific to satellite cells because they are also expressed in the cerebellum (21) and by hepatocytes (22). To specifically identify quiescent satellite cells, a

---

novel monoclonal antibody, SM/C-2.6, has recently been established (23). Satellite cells purified with this antibody regenerate muscle fibers on implantation into mdx mice (15).

The use of satellite cells for clinical therapies would require the establishment of a reliable source of these cells. Embryonic stem (ES) cells are totipotent stem cells that are able to differentiate into various types of somatic cells *in vitro*. While mouse embryonic stem (mES) cells can be readily induced to differentiate into muscle fibers (24, 25) and the myogenicity of human ES cells was recently validated (26), the induction of mES cells into functional satellite cells has not been reported. Here we have successfully induced mES cells to generate cells expressing Pax7 *in vitro* by forming embryoid bodies (EBs). These ES cell-derived (ES-derived) Pax7-positive cells can be enriched using the SM/C-2.6 antibody (23) and possess a great potential for generating mature skeletal muscle fibers both *in vitro* and *in vivo*. The Pax7-positive cells display a self-renewal ability that can repopulate Pax7-positive cells *in vivo* in the recipient muscles following an injury. Furthermore, these ES-derived Pax7-positive cells could engraft in the recipient muscle for long periods, up to 24 wk, and could also be serially transplanted. These results indicate that ES-derived Pax7-positive cells possess satellite cell characteristics. This is the first report of effective induction of functional satellite cells from mES cells, and these novel findings may provide a new therapeutic approach for treatment of DMD.

MATERIALS AND METHODS

Cell culture

D3 cells, mES cells (27) that ubiquitously express the *EGFP* gene under the *CAG* promoter (28) (a gift from Dr. Masaru Okabe, Osaka University, Osaka, Japan), were used in this study. ES cells were maintained on tissue culture dishes (Falcon) coated with 0.1% gelatin (Sigma, Oakville, CA, USA), in DMEM (Sigma) supplemented with 15% fetal bovine serum (FBS; Thermo Trace, Melbourne, Australia), 0.1 mM 2-mercaptoethanol (Nakalai Tesque, Japan), 0.1 mM nonessential amino acids (Invitrogen, Burlington, CA, USA), 1 mM sodium pyruvate (Sigma), penicillin/streptomycin (50 µg/mL), and 5000 U/ml leukemia inhibitory factor (Dainippon Pharmaceutical Co., Japan).

In vitro differentiation of ES cells into a muscle lineage

To induce EB formation, undifferentiated ES cells were cultured in hanging drops for 3 d at a density of 800 cells/20 µl of differentiation medium, which consisted of DMEM supplemented with penicillin/streptomycin, 0.1 mM nonessential amino acids, 0.1 mM 2-mercaptoethanol, 5% horse serum (HS), and 10% FBS. EBs were transferred to suspension cultures for an additional 3 d (d 3+3). Finally, the EBs were plated in differentiation medium in 48-well plates (Falcon) coated with Matrigel (BD Bioscience, Bedford, MA, USA). The medium was changed every 5 d.

Immunofluorescence and immunocytochemical analysis

Immunostaining of cultured cells and recipient mouse tissues were carried out as described previously (29). Briefly, the left tibialis anterior (LTA) muscle of the recipient mouse was fixed with 4% paraformaldehyde and cut into 6 µm cross sections using a cryostat, and samples were fixed for 5 min in 4% paraformaldehyde (PFA) in PBS and permeabilized with 0.1% Triton X-100 in PBS for 10 min. After incubation in 5% skim milk for 10 min at room temperature to block nonspecific antibody binding, cells were incubated for 12 h at 4°C with anti-mouse monoclonal antibodies. Antibodies used in this study were mouse anti-Pax7, which was biotinylated using a DSB-X Biotin Protein Labeling Kit (D20655; Molecular Probes, Eugene, OR, USA), mouse anti-Pax3 (MAB1675, MAB2457; R&D Systems, Minneapolis, MN, USA), rabbit anti-mouse Myf5 (sc-302; Santa Cruz Biotechnology, Santa Cruz, CA, USA), mouse anti-mouse M-cadherin (205610; Calbiochem, San Diego, CA, USA), mouse anti-myosin heavy chain (MHC; 18-0105; Zymed Laboratories, San Francisco, CA, USA; reacts with human, rabbit, rat, mouse, bovine, and pig skeletal MHC), mouse anti-mouse myogenin and mouse anti-mouse Myo-D1 (M3559, M3512; Dako, Carpinteria, CA, USA), monoclonal rabbit anti-mouse laminin (LB-1013; LSL, Tokyo, Japan), and mouse anti-mouse dystrophin (NCL-DYS2; Novocastra Laboratories, Newcastle-upon-Tyne, UK). Cy3-labeled antibodies to mouse or rabbit IgG, fluorescein isothiocyanate-labeled antibodies to mouse or rabbit IgG (715-005-150, 711-165-152; Jackson ImmunoResearch Laboratory, Bar Harbor, ME, USA), or Alexa 633-labeled goat anti-rabbit IgG (A21070; Invitrogen, Molecular Probes) were applied as secondary antibodies. Hoechst 33324 (H3570; Molecular Probes) was used for nuclear staining. The samples were examined with a fluorescence microscope (Olympus, Tokyo, Japan) or an AS-MDW system (Leica Microsystems, Wetzlar, Germany). Micrographs were obtained using an AxioCam (Carl Zeiss Vision, Hallbergmoos, Germany) or the AS-MDW system (Leica Microsystems). In sections of muscles transplanted with ES-derived satellite cells, the number of GFP-positive muscle fascicles and GFP/Pax7-double-positive cells were counted, per field, at ×100. More than 10 fields in each tissue sample were observed. To prevent nonspecific secondary antibody binding to Fc receptors, all immunostaining of frozen sections used the Vector® M.O.M™ Immunodetection Kit (BMK-2202; Vector Laboratories, Burlingame, CA, USA).

PCR analysis

Total RNA was isolated from cultured cells in 48-well plates, using TRIzol reagent (Invitrogen). The following specific primers were used for PCR:

Pax3, sense, 5′-AACACTGGCCCTCAGTGAGTTCTAT-3′, and antisense, 5′-ACTCAGGATGCCATCGATGCTGTG-3′; Pax7, sense, 5′-CATCCAGTGCTGGTACCCCACAG-3′, and antisense, 5′-CTGTGGATGTCACCTGCTTGAA-3′; Myf5, sense, 5′-GAGCTGCTGAGGGAACAGGTGG-3′, and antisense, 5′-GTTCTTTCGGGACCAGACAGGG-3′; MyoD, sense, 5′-AGGCTCTGCTGCGCGACCAG-3′, and antisense, 5′-TGCAGTCGATCTCTCAAAGC-3′; myogenin, sense, 5′-TGAGGGAGAAGCGCAGGCTCAAG-3′, and antisense, 5′-ATGCTGTCCACGATGGACGTAAGG-3′; M-cadherin, sense, 5′-CCACAAAACGCCTCCCCTACCC-3′, and antisense, 5′-GTCGATGCTGAAGAACTCAGGGC-3′; C-met, sense, 5′-GAATGTCGTCCTACACGGCCAT-3′, and antisense, 5′-CACTACACAGTCAGGACACTGC-3′; GAPDH, sense, 5′-TGAAGGTCGGTGTGAACGGATTTGGC-3′, and antisense, 5′-TGTTGGGGGCCGAGTTGGGATA-3′. AmpliTaqGold (Applied

Biosystems, Foster City, CA, USA) was used for PCR amplification. The amplification program used was 35 cycles of 30 s at 94°C, 30 s at 64°C, and 40 s at 72°C, with a final incubation of 7 min at 72°C.

Flow cytometry and cell sorting

Cultured cells were incubated with enzyme-free Hank's-based Cell Dissociation Buffer (Invitrogen) for 30 min at 37°C and gently dissociated into single cells. The cells were then washed with PBS twice, probed with biotinylated-SM/C-2.6 (23) antibody for 15 min at room temperature, and stained with phycoerythrin-conjugated strepavidin (12-4312; eBioscience, San Diego, CA, USA) for 15 min at room temperature. Dead cells were excluded from the plots based on propidium iodide staining (Sigma), and SM/C-2.6-positive cells were collected using a FACS Vantage instrument (Becton Dickinson, San Jose, CA, USA). Sorted cells were plated (1×10^4 cells/well) with differentiation medium in 96-well plates (Falcon) coated with Matrigel (008504; BD Bioscience). The medium was changed every 5 d, and 7 d after plating the cultured cells were analyzed.

Intramuscular cell transplantation (primary transplantation)

Recipient mice were injected with 50 µl of 10 µM cardiotoxin (CTX; Latoxan, Valence, France) (30) in the LTA muscle 24 h before transplantation (31). CTX is a myotoxin that destroys myofibers, but not satellite cells, and leaves the basal lamina and microcirculation intact. Since proliferation of host myogenic cells may prevent the incorporation of transplanted cells, recipient mdx mice (15) received 8 cGy of systemic irradiation (32) 12 h before transplantation to block muscle repair by endogenous cells. An average of 4.53×10^4 ES-derived SM/C-2.6-positive or -negative cells were washed twice with 500 µl of PBS, resuspended in 20 µl of DMEM, and injected into the LTA muscle of recipient mdx mice using an allergy syringe (Becton Dickinson). Mdx mice, which are derived from the CL/B16 strain, were used as the recipient mice in all experiments. Similarly, D3 ES cells, which are derived from the 129X1/SvJ ES cells, were used in all experiments. The major histocompatibility complex (MHC) of mdx mouse and D3 cells are very similar, both possessing type b MHC H2 haplotypes. All animal-handling procedures followed the Guild for the Care and Use of Laboratory Animals published by the U.S. National Institutes of Health (NIH Publication No. 85-23, revised 1996) and the Guidelines of the Animal Research Committee of the Graduate School of Medicine, Kyoto University.

Secondary transplantation

The LTA muscles of recipient mice were collected 8 wk after the primary transplantation. The muscles were minced and digested into single cells with 0.5% collagenase type I (lot S4D7301; Worthington Biochemical Corp., Lakewood, NJ, USA). After washing with PBS and filtration through a 100 µm filter, Pax7-positive cells were sorted by FACS using the SM/C-2.6 antibody. SM/C-2.6-positive cells (200 cells/mouse) were injected into preinjured LTA muscles of secondary recipient mice. The LTA muscles were analyzed 8 wk after transplantation.

Isolation and immunostaining of single fibers

To detect muscle satellite cells attaching to single fibers with Pax7, muscle fibers from the LTA muscle of recipient mice

were prepared essentially according to the method of Bischoff in Rosenblatt *et al.* (33). Briefly, dissected muscles were incubated in DMEM containing 0.5% type I collagenase (Worthington) at 37°C for 90 min. The tissue was then transferred to prewarmed DMEM containing 10% FBS. The tissue was gently dissociated into single fibers by trituration with a fire-polished wide-mouth Pasteur pipette. Fibers were transferred to a Matrigel-coated 60 mm culture dish (Falcon) and fixed in 4% PFA for 5 min at room temperature. Fibers were permeabilized with 0.1% Triton X-100 in PBS for 10 min, and nonspecific binding was blocked by incubation in 5% skim milk for 10 min at room temperature. Primary mouse monoclonal antibodies against mouse Pax7 were applied for 12 h at 4°C. Antibodies were detected using the secondary antibodies described above.

Statistics

Data are presented as means ± SD. For comparison of the numbers of MHC and Pax7-positive cells in the sorted SM/C-2.6-positive and -negative fractions and the numbers of GFP-positive muscle fascicles and GFP/Pax7-double-positive cells in reinjured and noninjured groups, the unpaired Student's *t* test was used, and a value of $P < 0.05$ was considered to be statistically significant.

RESULTS

Myogenic lineage cells are effectively induced from mES cells *in vitro*

EBs were formed in hanging drop cultures for 3 d followed by an additional 3 d in suspension cultures (**Fig. 1A**). These EBs were then plated onto Matrigel-coated 48-well plates in differentiation medium, which contained 5% HS. This culture method is a modified version of the classical ES cell differentiation method (25) and the skeletal muscle single fiber culture method (33). After plating, EBs quickly attached to the bottom of the coated dishes, and spindle-shaped fibers appeared surrounding the EBs by the seventh day of plating (d 3+3+7; Fig. 1B). As these spindle fibers grew, they began to fuse with each other, forming thick multinucleated fibers resembling skeletal myofibers (Fig. 1C, D). At the same time we observed spontaneous contractions by the fibers (Supplemental Videos 1 and 2), a trait commonly seen in cultured skeletal muscle fibers. Immunostaining showed that these fused fibers were positive for skeletal-muscle-specific MHC (Fig. 1E). Furthermore, cells expressing muscle regulatory factor (MRF) proteins, including Pax7 (Fig. 1F), Myf5 (Fig. 1G), MyoD (Fig. 1H), and myogenin (Fig. 1I) were observed. On d 3 + 3 + 14, the average number of MHC-positive wells was 73.6 ± 5.8% (*n*=144). In all the MHC-positive wells, cells expressing Pax7, an essential transcription factor in satellite cells, were also observed. Double staining for Pax7 and MyoD confirmed the existence of cells staining for Pax7 alone, indicating the presence of quiescent-state satellite cells (34) within the culture (Supplemental Fig. 1). Next, the time course of MRF expression was examined by RT-PCR (Fig. 1J). Expression of Pax3 and Pax7 both peaked on d 3 + 3 +